Processes in Heavy Element Nucleosynthesis

Saumi Dutta
Department of Physics, University of Calcutta,
92, Acharya Prafulla Chandra Road,
Kolkata - 700009, India
email: saumidutta89@gmail.com

Introduction

Slow neutron capture process (s-process) produces about half of the heavy elements beyond iron. The s-process proceeds along the valley of nuclear stability via the interplay of neutron capture and β-decay. It is subdivided into weak and main components. The nuclei in the mass range $56 \leq A < 90$ are produced in the weak component. The isotopes with $A > 90$ are produced in the main component that occurs in radiative conditions during the interpulse phases of subsequent He shell burning in the thermally pulsating asymptotic giant branch (TP-AGB) stars of masses in between $1 \leq M/M_{\odot} \leq 3$ ($M_{\odot}$ being the solar mass). Neutrons are released in two reactions, one is $^{13}\mathrm{C}(\alpha, n)$ and another is $^{22}\mathrm{Ne}(\alpha, n)$. However, the $^{22}\mathrm{Ne}(\alpha, n)$ reaction is only marginally activated in low mass AGB stars during the last few thermal pulses.

Abundances in s-process are determined by solving a complex network consisting of a set of coupled differential equations. Radiative neutron capture rates are the basic inputs in the s-process network calculation. However, (n, γ) cross sections/ rates pertinent to s-process cannot be measured at all astrophysical energies and for all relevant isotopes. Hence, one must fill the existing gaps in experimental data from a moderate statistical model. In the present thesis, a statistical model, based on the compound nuclear Hauser-Feshbach framework, has been constructed. The (n, γ) cross sections as well as reaction rates over a range of s-process energies and temperatures have been calculated with this statistical model using the reaction code TALYS [1] for nuclei residing in and around various proton and neutron shell-closures, in particular near the $Z = 28$, $N = 50$, $Z = 50$, and $N = 82$ shell-closures in the s-process path.

Model framework

The complex optical model potential (OMP), that divides the incident flux into two channels, one describing elastic scattering and another describing reaction, is the major ingredient in the statistical Hauser-Feshbach model. In the present work, a semi-microscopic complex optical model potential has been formulated by folding the effective density-dependent M3Y (DDM3Y) nucleon-nucleus interaction [2] with the target radial matter densities $\rho(\mathbf{r}')$. The matter densities have been extracted from our relativistic-mean-field (RMF) model based on the FSUGold Lagrangian density [3].

$$V_{fold} = \int V_{NN}|\mathbf{r} - \mathbf{r}'|\rho(\mathbf{r}')d\mathbf{r}' \qquad (1)$$

DDM3Y is a real interaction. The imaginary component in the OMP that describes reaction channels is taken identical to the real part. The real and imaginary potential well-depths are normalized with the constants N_r and N_{im} that are assigned the values = 1 for the entire calculation. The final form of the optical potential is given as,

$$V_{omp} = N_r V_{fold} + N_{im} V_{fold} \qquad (2)$$

Nuclear level densities and E1 γ-ray strength functions, the essential ingredients for Hauser-Feshbach model, are taken from the latest microscopic calculations [4–6]. Details of the calculations are available in Refs. [7–10].

Next, we have built up and solved a large network for s-process where we have utilized the statistical model (n, γ) rates as inputs. We have taken the time-varying neutron densities provided by $^{13}\mathrm{C}(\alpha, n)$ reaction from Gallino *et. al.* [11] corresponding to neutron exposures 0.23 and 0.41 mb^{-1}. Thereafter, we have enhanced the neutron exposures by multiplying them with a factor 1.5. A typical time-variation of temperature for an inter-pulse period of 20000 years, computed by stellar evolutionary code FRANEC [12], has been taken from Lugaro *et. al.* [13] in the present work. Total 12 iron group nuclei with solar abundances are taken as seeds. Finally, we have studied the sensitivity for (n, γ) rates to identify the reactions that have the strongest global impact on s-process abundance in the main component. Sensitivity (s_{ij}) is defined as the ratio of the relative change in abundance of isotope j to the relative change in the rate of isotope i; $s_{ij} = \frac{\Delta N_j/N_j}{\Delta r_i/r_i}$. Hence, sensitivity gives the coupling between the change in the reaction rate and the change in final abundances.

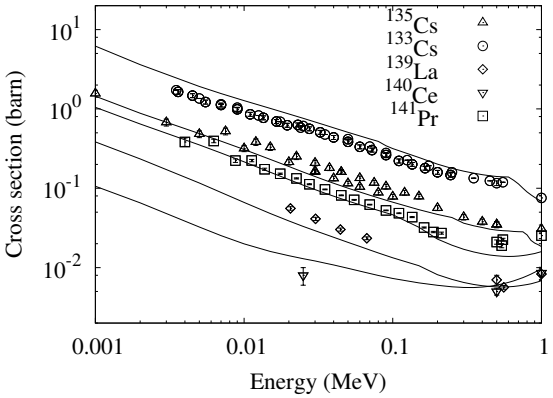

FIG. 1: Comparison of results of the present calculation (solid lines) with experimental measurements for ^{133,135}Cs, ^{139}La, ^{140}Ce, and ^{141}Pr.

Results

In Fig. 1, the (n, γ) cross sections of ^{133,135}Cs, ^{139}La, ^{140}Ce, and ^{141}Pr from 1 keV to 1 MeV are com-

TABLE I: The isotopes, the (n,γ) rates of which show strong sensitivity during the s-process in the ^{13}C pocket. The second column represents the total number of affected isotopes in the s-process path with sensitivity $(s_{ij}) \geq \pm 0.1$ due to a change in 20% in each rate. The last column distinguishes the isotopes on the basis of their location in the s-path around various neutron and proton shell-closures.

Nucleus	No.	Location	Nucleus	No.	Location
^{56}Fe	178	$Z = 28$	^{62}Ni	165	$Z = 28$
^{88}Sr	146	$N = 50$	^{58}Fe	134	$Z = 28$
^{60}Ni	126	$Z = 28$	^{68}Zn	111	$Z = 28$
^{90}Zr	100	$N = 50$	^{138}Ba	82	$N = 82$
^{140}Ce	81	$N = 82$	^{89}Y	73	$N = 50$

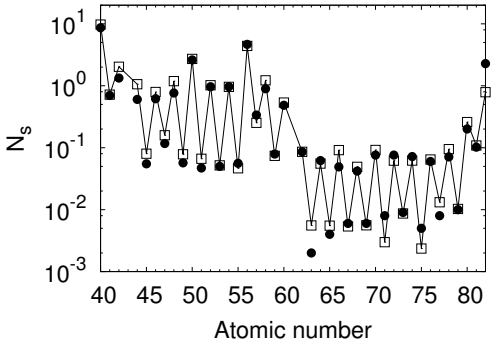

FIG. 2: Elemental abundance distribution from Zr to Pb. Abundances are normalized to Sm peak. The squares connected by solid line represents our calculations and the circles denote s-contribution to total solar abundance from classical model analysis taken from Cowan *et. al.* [14].

pared with the latest experimental data. Experimental cross section values for ^{133,135}Cs(n,γ) reaction are from Refs. [15–17]. The data for ^{139}La are from Refs. [17, 18] while for ^{140}Ce are from Ref. [19]. For ^{141}Pr, the measurements are from Ref [19, 20]. It can be seen that the agreement between the statistical model calculations and experimental values are reasonable. This suggests the feasibility and reliability of the model. The predictions from our RMF model, such as binding energies, charge density profiles, and root-mean-square charge radius values have been compared with experimental data, whenever available. However, to limit the length, the results cannot be presented. They are available in Refs. [7–10]. These comparisons suggest the reasonable predictive power of the RMF model.

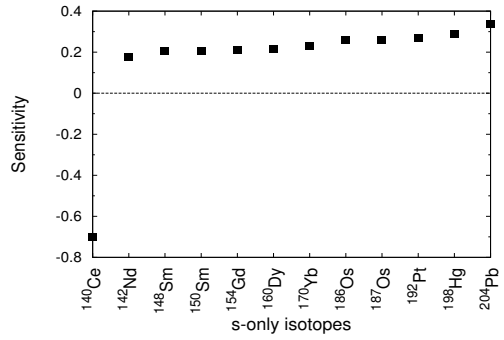

FIG. 3: Sensitivities for the magic bottleneck reaction ^{140}Ce(n,γ) are plotted only over the s-only isotopes as well as for ^{140}Ce for the reasons of clarity. The change in the (n,γ) rate of ^{140}Ce does not affect the isotopes preceding it and hence, for the clarity in view, the preceding isotopes are not shown.

In Fig. 2, the elemental s-process abundance distribution from Zr to Pb, obtained from the present network calculations, has been compared with the classical s-process model prediction [14]. This figure shows that the above choice of the ^{13}C neutron exposures yield a reasonable agreement with the solar s-process abundance values for the main component.

For the sensitivity analysis, the (n,γ) rate of each isotope has been changed individually by 20% and the corresponding changes in isotopic abundances are observed. The degree of sensitivity is determined by the number of affected isotopes over a threshold of $s_{ij} = \pm 0.1$. We have found that among all the neutron capture reactions, only a few have a significant global impact over the entire abundance distribution. They are listed in Table I. The impact is determined by the number of affected isotopes over a threshold value of $s_{ij} = \pm 1$. The interesting fact is that, these rates are for the reactions on magic nuclei acting as bottlenecks to the s-process reaction flow. Fig. 3 shows the sensitivity of ^{140}Ce(n,γ) reaction rate over the s-only isotopes. It can be seen that an increased rate increases the production of the isotopes following ^{140}Ce at the cost of its own abundance. Further, on the basis of the sensitivity study, the most important reaction rates for each isotope are identified. The impact of statistical model (n,γ) rates, obtained with different optical model potentials, have also been studied. However, due to the limitation in length, these results cannot be shown here.

Acknowledgment

Author acknowledge the University Grants Commission (India), Departmental Research Scheme of University of Calcutta (India), and the Alexander-von-Humboldt Foundation (Germany) for financial assistance.

References

[1] A. J. Koning *et. al.*, Proc. of the Int. Conf. on Nucl. Data for Sci. and Tech., Nice, France, April 22–27, 2007; www.talys.eu
[2] G. R. Satchler *et. al.*, Phys. Rep. **55**, 183 (1979).
[3] B. Todd-Rutel *et. al.*, Phys. Rev. Lett. **95**, 122501 (2005).
[4] S. Goriely *et. al.*, Phys. Rev. C **78**, 064307 (2008).
[5] S. Goriely *et. al.*, Nucl. Phys. A **739**, 331 (2004).
[6] S. Goriely, Phys. Lett. B **436**, 10, (1998).
[7] S. Dutta *et. al.*, arxiv: 1610:02677 [nucl-th].
[8] S. Dutta *et. al.*, Phys.Rev.C **94**, 054611 (2016).
[9] S. Dutta *et. al.*, Phys.Rev.C **93**, 024602 (2016).
[10] S. Dutta *et. al.*, Phys.Rev.C **94**, 024604 (2016).
[11] R. Gallino *et. al.*, Ap. J. **497**, 388 (1998).
[12] A. Chieffi *et. al.*, Ap. J. Supp. Ser. **71**, 47 (1989).
[13] M. Lugaro *et al.*, Ap. J. **586**, 1305 (2003).
[14] J. J. Cowan *et. al.*, Invited talk, NASA LAW, UNLV, Las Vegas, February 14–16, 2006.
[15] R. Macklin, Nucl. Sci. and Eng. **89**, 79 (1985).
[16] N. Yamamuro *et. al.*, Jour. Nucl. Sci. Tech. **20** 797 (1983).
[17] J. Voignier *et. al.*, Nucl. Sci. and Eng. **112**, 87 (1992).
[18] M. Igashira *et. al.*, Nucl. Data for Sci. and Tech. **2**, 1299 (2007).
[19] S. Harnood *et. al.*, Jour. Nucl. Sci. and Tech. **37**, 740 (2000).
[20] F. Voss *et. al.*, Phys. Rev. C **59**, 1154 (1994).